

General Disclaimer

One or more of the Following Statements may affect this Document

- This document has been reproduced from the best copy furnished by the organizational source. It is being released in the interest of making available as much information as possible.
- This document may contain data, which exceeds the sheet parameters. It was furnished in this condition by the organizational source and is the best copy available.
- This document may contain tone-on-tone or color graphs, charts and/or pictures, which have been reproduced in black and white.
- This document is paginated as submitted by the original source.
- Portions of this document are not fully legible due to the historical nature of some of the material. However, it is the best reproduction available from the original submission.

MECHANICAL AND CHEMICAL EFFECTS OF
ION-TEXTURING BIOMEDICAL POLYMERS

(NASA-TM-79245) MECHANICAL AND CHEMICAL
EFFECTS OF ION-TEXTURING BIOMEDICAL POLYMERS
(NASA) 29 p HC A03/MF A01

CSCL 07C

N79-31391

G3/27

Unclassified
35771

A. J. Weigand and M. A. Cenkus
Lewis Research Center
Cleveland, Ohio



Prepared for the
Thirty-second Annual Conference of Engineering
in Medicine and Biology
sponsored by the Alliance for Engineering in Medicine
Denver, Colorado, October 6-10, 1979

MECHANICAL AND CHEMICAL EFFECTS OF ION-TEXTURING
BIOMEDICAL POLYMERS

by A. J. Weigand and M. A. Cenkus
National Aeronautics and Space Administration
Lewis Research Center
Cleveland, Ohio 44135

ABSTRACT

To determine whether sputter-etching may provide substantial polymer surface texturing with insignificant changes in chemical and mechanical properties, an 8-cm-beam diameter, electron-bombardment, argon-ion source was used to sputter-etch (ion-texture process) nine biomedical polymers. The materials included silicone rubber, 32% carbon-impregnated polyolefin, polyoxymethylene, polytetrafluoroethylene, ultrahigh molecular weight (UHMW) polyethylene, UHMW polyethylene with carbon fibers (10%), and several polyurethanes (bioelectric, segmented, and cross-linked). Ion-textured microtensile specimens of each material except UHMW polyethylene and UHMW polyethylene with 10% carbon fibers were used to determine the effect of ion-texturing on tensile properties. Scanning electron microscopy was used to determine surface morphology changes, and electron spectroscopy for chemical analysis (ESCA) was used to analyze the near-surface chemical changes that result from ion-texturing.

Ion energies of 500 eV with beam current densities ranging from 0.08 to 0.19 mA/cm² were used to ion-texture the various materials. Standard microtensile specimens of seven polymers were exposed to a saline environment for 24 hours prior to and during the tensile testing. Tensile results showed that ion-texturing reduces the average ultimate strength from as little as 1% for segmented polyurethane to as much as 19% for polyoxymethylene.

Analysis of the full ESCA spectrum of the ion-textured samples indicated detectable amounts of argon imbedded into the surface of all samples except 32% carbon impregnated polyolefin and polytetrafluoroethylene. For polyoxymethylene, polyolefin, and the three polyurethanes the amount of oxygen relative to the carbon was reduced after ion-texturing. The two polyethylene samples showed an increase in the amount of oxygen relative to carbon after ion-texturing. In general it is concluded that the surface chemical changes resulting from sputter-etching are minimal in spite of the often significant changes in the surface morphology.

INTRODUCTION

One factor which affects the biological tissue response to an implant material is the surface morphology of the material (refs.

1 and 2). Most surface morphologies that have been investigated have a distribution of surface pore sizes (vitreous carbon (ref. 3), porous polyolefin (ref. 4)), which may cause nonuniform tissue response to various parts of the implant. Pores too small will not allow cell ingrowth. Other pores that interconnect too far under the surface will allow tissue ingrowth without proper nutrition, causing inflammation and, if severe enough, necrosis. A technique which uses technology developed from the National Aeronautics and Space Administration's electric propulsion program has been used to obtain controlled surface morphologies with well defined dimensions (ref. 5). By using implants with known surface roughnesses, a systematic investigation can be performed to evaluate the tissue response to surface morphology. An optimum implant surface texture for bone, soft tissue, or thrombus attachment can be deduced from in vivo tests of implants with controlled, precise surface morphologies.

To determine the effect of sputter-etching on the near-surface chemistry and bulk tensile properties, an electron-bombardment, ion thruster was used as a neutralized-ion-beam source to modify surface morphology of biomaterials (refs. 5 to 8). A beam of directed, energetic ions, produced by an ion source, can alter the surface morphology and/or chemistry of many materials (metals, polymers, ceramics). The process of sputter roughening or ion-texturing (ref. 9) involves the selective removal of atoms, molecules, or molecular fragments from the surface of a target material. Because each element has a certain and often different sputtering rate or because there is inhomogeneity within the material (crystalline and amorphous regions), the surface morphology usually will change as a result of ion sputtering. The surface chemistry is also very likely to change. Thus, the biological response to an ion-textured surface may be significantly different from the response to an untextured surface because of changes in morphology (ref. 10) and/or chemistry (ref. 11).

The transfer of energy from the impinging ions to the target material results in localized heating of the material. Many polymers are heat sensitive such that their bulk mechanical or chemical properties degrade as a consequence of being heated. The results of ion-texturing a polymer surface which often produces a submicron and micron size roughness may also alter the mechanical properties. Therefore, an investigation was undertaken to determine the extent of near-surface chemical changes and tensile property changes resulting from ion-texturing.

Nine biopolymers were examined. They included silicone rubber (Silastic), 32% carbon-impregnated polyolefin, polyoxymethylene (Delrin), polytetrafluoroethylene (Teflon), ultrahigh-molecular weight (UHMW) polyethylene, UHMW polyethylene with carbon fibers (10%), bioelectric polyurethane, segmented polyurethane (Biomer),

and cross-linked polyurethane (Tecoflex). Ion-textured, standard microtensile specimens of each material (except UHMW polyethylene and UHMW polyethylene with carbon fibers (10%) for which no tensile data were obtained) were used to determine the effects of ion-texturing on tensile properties. For all materials scanning electron microscopy was used to examine surface morphology changes, and electron spectroscopy for chemical analysis (ESCA) was used to analyze the near-surface chemical compositional changes that result from ion-texturing.

All the sputter-etching and SEM observations were performed at the Lewis Research Center. The tensile testing apparatus was the property of Case Western Reserve University, and these tests were performed in the Mechanical Engineering Department laboratory. ESCA determination was performed separately by Surface Science Laboratories under NASA contract and by Dr. David Dwight at Virginia Polytechnic Institute and State University under a NASA grant.

APPARATUS AND PROCEDURE

Ion-Texturing

An 8-cm-diameter ion source utilizing argon as the working gas was used to ion-texture all the polymers reported herein. This type of ion source can also operate with any of the inert gases, nitrogen (ref. 8), freons (ref. 12), and other gases. The ion source is used in a vacuum system with pressures ranging from 1.3×10^{-3} to 4×10^{-5} pascal (1×10^{-5} to 3×10^{-7} torr).

A schematic drawing of an 8-cm-beam diameter ion source is shown in figure 1. The basic design of the ion source includes a ribbon cathode which, when heated, is the source of bombarding electrons used to ionize the working gas. The cathode is made of a triple-strand of 0.5-mm (0.020 in.) diameter tantalum wire which is coated with a low-work-function material, BaO. The BaO aids in the electron emission process. The electron emission is controlled by the amount of power applied to the cathode filament. The discharge chamber is the volume in which the cathode electrons ionize the working gas atoms. A concentric-cylinder anode, operating at approximately 40 V higher positive potential than the cathode, is used to attract the electrons. A magnetic field, provided by six to eight 0.6-cm (0.25-in.) diameter permanent bar magnets equally spaced around the ion source, increases the bombarding electron path length through the discharge chamber. By extending the path length, the probability of ionization increases. The multiple-aperture ion extraction system consists of two grids with concentric, circular holes (ref. 13). The screen grid (adjacent to the discharge chamber) operates at a positive high voltage (300 to 2000 V), while the accelerator grid operates

at a negative voltage (-200 to -1000 V). A neutralizer, which for this ion source is a heated loop of double-strand, tantalum wire coated with BaO, provides electrons to neutralize the extracted ion beam. There is very little (approximately 1%) recombination of ions and electrons. This directed, slightly divergent, bulk-neutralized ion beam can then be used to sputter target material. Ion current densities from less than 0.1 to 1 mA/cm² are produced by the 8-cm-diameter ion source. The maximum target area over which the ion current density is uniform (within 15% of maximum) is 3x3 cm at a distance of 20 cm (7.9 in.) from the accelerator grid plane of an 8-cm-diameter ion source. All samples were textured within this uniform current density area.

For this investigation the target samples were centered on the ion-beam axis and placed 20 cm from the accelerator grid plane. Each material was exposed to a 500 eV argon-ion beam for 1 hour. Table I lists the ion current densities to which each material was exposed. The ion current densities were selected to minimize ion impingement heating effects.

Target samples (2.5x2.5 cm) of each material were ion-textured separately. The thickness of the samples ranged from 0.51 mm for segmented polyurethane to 3.18 mm for UHMW polyethylene (table I). These samples were used for SEM analysis and ESCA. Five standard microtensile specimens (ASTM D638-76) of each material (except UHMW polyethylene and UHMW polyethylene with carbon fibers (10%) for which no tensile data were obtained) were ion-textured simultaneously. As shown in figure 2, only the gage length section of both sides of each specimen was ion-textured. These samples were exposed to the same ion-beam conditions as the square samples (table I).

Tensile Property Measurements

To determine the effects of ion-texturing on the tensile properties of each biopolymer investigated, five standard microtensile specimens made from untextured (control) material and five ion-textured specimens were tested. The width and thickness of each sample was measured and recorded. The samples were put in a saline solution (0.9% NaCl) for 24 hours prior to the tensile tests and were in a saline solution during the test. Figure 3 shows the tensile testing apparatus used for the tests. Each sample was placed in self-aligning grips according to standard procedures. The constant strain rates or crosshead speeds used were those suggested by the manufacturer of each material and are given in table II. A strip-chart recorder was used to record the stress-strain curve for each sample. Each sample was tested to failure. Several samples came loose from the grips before failure. These data were not included in the determination of tensile properties.

ESCA

ESCA was performed on samples of each material that were exposed to three environmental conditions. The first set of samples was untextured and used as a control. These samples were biodegradable-detergent cleaned in an ultrasonic cleaner. Another set of samples was similarly cleaned and exposed to the vacuum environment but not ion-textured. The third set of samples was cleaned and ion-textured in the same vacuum environment. By analyzing all three sets of samples, the separate effects of vacuum exposure and ion-texturing can be determined. The ESCA was performed by two independent laboratories (refs. 14 and 15) to obtain a consensus of opinion of the interpretation of results.

RESULTS AND DISCUSSION

Tensile Properties

Typical engineering stress-strain diagrams for untextured and ion-textured samples of silicone rubber, 32% carbon-impregnated polyolefin, polyoxymethylene, polytetrafluoroethylene, bioelectric polyurethane, segmented polyurethane, and cross-linked polyurethane are shown in figures 4 to 10, respectively. The average tensile strength at failure were also the ultimate tensile strength and is given in table II for untextured and ion-textured samples of each polymer. The percent reduction in tensile strength resulting from ion texturing is also given in table II. Ion-texturing reduces the ultimate strength from as little as 1% for segmented polyurethane to as much as 19% for polyoxymethylene. Because of sample to sample variation of the individual tensile strength data, as indicated by the range of variation given in table II, it can be concluded that the reduction of tensile strength after ion-texturing is not a significant change.

Both the untextured and ion-textured specimens of each polymer failed at the ultimate tensile strength. The general shape of the stress-strain curves for both untextured and ion-textured samples of all the polymers was the same. The two exceptions were polyoxymethylene (fig. 6) and polytetrafluoroethylene (fig. 7). The stress-strain curves for the ion-textured polyoxymethylene samples did not show an initial low elastic modulus deformation (large strain for small stress, ref. 16) which was characteristic of the untextured samples. The stress-strain curves for the polytetrafluoroethylene samples reveal an effect of ion-texturing that is similar the effect of increasing the bulk temperature (ref. 17).

SEM Photomicrographs

Figures 11 to 19 are scanning electron photomicrographs of the ion-textured polymer surfaces (textured under the conditions given

in table I). The carbon-impregnated polyolefin (fig. 12), bio-electric polyurethane (fig. 15), segmented polyurethane (fig. 16), and cross-linked polyurethane (fig. 17) develop a worm-like surface structure. Polyoxymethylene (fig. 13) and polytetra-fluoroethylene (fig. 14) develop a needle-or cone-like structure. Silicone rubber (fig. 11), UHMW polyethylene (fig. 18) and UHMW polyethylene with 10% carbon fibers (fig. 19) did not develop a pronounced surface roughness after ion-texturing.

ESCA

General results and discussion. - Detailed ESCA were done for each polymer subjected to three different treatments (control, vacuum exposure, and ion-textured). A survey ESCA spectrum of each sample indicated which elements were present. The photo-electrons, emitted from a surface as a result of X-ray excitation, have a certain small range of energy. For example, the C_{1s} electron has a nominal energy of 284 eV. The elements to which the carbon is attached will affect the energy. Thus, there may be several overlapping peaks (components) close to 284 eV which indicates that the carbon is attached to several elements. A high resolution spectrum for each element detected was then taken to assist in the interpretation of the overlapping peaks. The results of these analyses are given in tables III, IV, and V. The surface elemental compositions estimated from the data and expressed as atom percent for the detected elements are listed in table III for all polymers. The surface composition data were then renormalized to present the number of atoms of the major constituents relative to the total number of carbon atoms defined as 1.00 (table IV). When the photoelectron spectrum for an element showed more than one component, the region was fitted using a theoretical model which assumes Gaussian line shapes and a particular shape for the background. With this technique, each component or functional group is resolved.

The C(1s) spectrum fitting calculations produced estimates for the fraction of the total C(1s) intensity in each component and the binding energy and line width for each component. These C(1s) components are listed individually in table IV in addition to the O, N, F, and Si detected. The C(1s) components are listed C_a, C_b, C_c, and C_d in order of increasing binding energy. Thus, C_a is the heading for the C(1s) component at the lowest binding energy for each sample. This method of presenting the surface composition data emphasizes the ESCA information related to the organic components of the surface and the changes produced therein by the two treatments applied.

The third and final set of numerical data is the list of binding energies extracted from the spectra (table V). The binding energies are normalized so that the C_a component is set to 284.0

eV for each sample. General comments applicable to the entire sample set as well as specific comments on the apparent effect of the vacuum and ion texturing on specific polymers are given below.

From the data in tables III, IV, and V there are several observations of a general nature that deserve emphasis or special comment. The first point concerns the detection of argon for the ion-textured samples. All ion-textured samples except 32% carbon-impregnated polyolefin and PTFE showed detectable amounts of argon in the surface (probably either implanted or surface adsorbed).

Another general observation is that there appears to be only minor differences between the control and vacuum-exposed samples of each polymer. However, the ion-textured samples do appear to differ from the control and vacuum-exposed samples for many of the polymers. This fact is readily apparent in the oxygen/carbon portions (O/C) of the data. For the three polyurethanes, polyolefin, and polyoxymethylene the ion-texturing caused a reduction in the amount of oxygen relative to carbon. This reduction is particularly pronounced for polyoxymethylene where O/C dropped from 0.75 (control) to 0.16 (ion-textured). Ion-texturing increased the O/C for the two polyethylene samples.

A surface constituent element common to each of the polymer samples was silicon (Si). The detergent cleaning did not seem to affect the amount of Si detected to any great extent except for the polyoxymethylene sample. Ion-texturing did not seem to produce any significant change in the Si level either, except for polyethylene with 10% carbon fiber and polyolefin. Both of these samples had in common the fact that elemental carbon was listed as a component of the material.

Among the hydrocarbon polymers, only UHMW polyethylene shows a pronounced chemical effect after ion-texturing (ref. 10). Oxidation appears to be introduced after ion-texturing. The oxygen concentration increases and an oxidized carbon peak arises. The ion-texturing effects on surface morphology are far more pronounced than the effects on surface chemistry. Moreover, roughening the surface reduces the depth of penetration of ESCA, thereby emphasizing the functional groups in the top surface layers. For UHMW polyethylene, which did not develop much of a surface texture (fig. 18), the chemical changes after ion-texturing indicated by ESCA analysis should be representative of the gross surface structure.

The near-surface chemical composition of the polyurethanes is not drastically changed by the ion beam. Each of the polyurethanes may have been reduced (decrease in oxygen content) by the ion beam.

Polyoxymethylene shows the most dramatic chemical changes, but this effect may be related to the fact that this polymer shows the most pronounced ion-roughening. PTFE shows a small increase in hydrocarbon after ion-texturing.

The two separate laboratory ESCA results showed good agreement with regard to these general comments. However, there were slight differences which may have been due to sample preparation or shipment. Therefore, the discussion of the ESCA of each polymer will be based on one set of data (ref. 11).

Specific comments for each polymer.

1. Bioelectric polyurethane. - The C(1s) spectrum for the control sample of this set shows three components which can be assigned to carbon bonded to other carbon or hydrogen (C_a), carbon singly bonded to oxygen (C_b), and carbon doubly bonded to oxygen (C_c). For the vacuum-exposed sample the C(1s) spectrum is similar to that for the control sample except that there is a fourth carbon peak, C_d. Also, detectable amounts of fluorine were noted. These observations suggest that C_d for the vacuum-exposed sample be assigned to a fluorocarbon surface contaminant.

The C(1s) spectrum for the ion-textured sample showed a lower intensity for peak C_b (relative to C_a) than was found for the control and vacuum-exposed samples. This result is concomitant with a smaller amount of oxygen for the ion-textured sample. The amount of nitrogen detected was lower by about a factor of 2 for the ion-textured sample as compared with the control and vacuum-exposed samples. These changes suggest that after ion-texturing the surface is no longer identical to the surface before ion-texturing. The principal difference appears to be a greater amount of C_a relative to other features, which reflect the functional groups expected for polyurethane.

Spectrum for the ion-textured sample showed signals assigned to argon, sulfur, and iridium not detected for the other samples in the set. The detection of signals assigned to Ir was considered unusual. No other assignment could be given these signals which would match all the data, however.

2. Segmented polyurethane (Biomeric). - The C(1s) spectra are qualitatively similar to those recorded for bioelectric polyurethane, and the assignment of the components is the same. The survey spectra of the three samples of this polymer are very similar, indicating that the ion-texturing had little effect on the surface chemical composition. The ion-textured sample did show a smaller amount of oxygen, which was concomitant with a lower amount of silicon. It may be that the lower oxygen content after ion-texturing is due to a reduction in the amount of silicon/oxygen containing material present at the surface. Also, the control and

vacuum-exposed samples showed significant amounts of S and Cl while the ion-textured sample showed only a minor amount of Cl and no detectable S. Iron was detected for the control and vacuum-exposed samples and fluorine was detected for the ion-textured sample only.

3. Polyoxymethylene (Delrin). - The C(1s) spectra for the control and vacuum-exposed samples of this set are qualitatively similar. There are two distinct components separated by about 2 eV. Peak C_b is the carbon associated with the C-O group of the polyoxymethylene structure while C_a must arise from an additive or surface contaminant. Note that the atom ratio C_b/O is very close to 1.00 for both the control and vacuum-exposed samples as would be expected for the polyoxymethylene structure.

The ion-textured sample of this set is very different from the other two. The O/C atom ratio dropped from 0.75 to 0.16 after ion-texturing. The C(1s) spectra show a strong peak at the position expected for carbon bonded to other carbon or hydrogen, but only a weak peak at the position expected for the C-O group of polyoxymethylene. Apparently, the ion-texturing has reduced the surface of the polymer or led to the deposition of a hydrocarbon on the sample surface. Of the nine polymers studied, polyoxymethylene shows the most drastic differences between the ion-textured and untextured surfaces.

4. UHMW polyethylene. - The C(1s) spectra for this set show a strong line associated with the polyethylene carbon and weaker lines on the high binding energy side which arises from carbon-oxygen functional groups. These peaks are small, and it is difficult to extract much useful information concerning intensities or positions from the C(1s) spectra. It is clear, however, that the ion-textured sample shows both a higher oxygen content and a greater intensity in the C-O peaks. It can be concluded that ion sputtering produces a surface richer in oxygen and C-O functional groups than the untextured samples.

All three spectra of the samples of this set showed Si and Mg signals. The ion-textured sample spectrum showed a quite intense line for Zn not detected for either nonspattered samples.

5. UHMW polyethylene with 10% carbon fibers. - Each of the samples showed an intense main C(1s) peak associated with the polyethylene carbons plus much weaker and less well-defined components associated with C-O functional groups. The ion sputtered sample spectrum showed slightly more oxygen than did the other two nonspattered samples.

6. 32% carbon-impregnated polyolefin. - The C(1s) spectra for the samples of this set show an intense peak associated with the

polyolefin carbons. All three of these samples showed detectable amounts of oxygen with the ion-textured sample exhibiting the lowest oxygen value. Zinc, S, and F were found for each sample.

7. Silicone rubber (Silastic). - The ESCA data indicate that this silicone is dimethyl silicone. There are slight differences between the samples which may not be significant. The only elements detected in addition to C, Si, and O were S and Ar for the ion sputtered sample.

8. Cross-linked polyurethane (Tecoflex). - The results for this set are very similar to those for bioelectric polyurethane (1). The C(1s) spectra show the same structure, the O/C ratios are essentially the same, and Si is a common surface contaminant. However, Sn was detected for all three samples. In addition, quite large amounts of fluorine were found for the vacuum-exposed sample concomitant with the appearance of a fourth carbon peak in the C(1s) spectrum. This peak is assigned to carbon present as fluorocarbon. The appearance of fluorine may be due to fluoropolymer from vacuum tank wall deposits.

9. Polytetrafluoroethylene (Teflon). - The spectra for the control and vacuum-exposed samples are typical of PTFE. The principal C(1s) peak at 291.4 eV (C_p) arises from the CF_2 group carbon. Note that the F/C_p atom ratio is 2.07 for the control sample and 2.09 for the vacuum exposed sample. For the ion-textured sample the C(1s) spectrum is more complex with several weak components. These weaker components are also assigned to carbon atoms bonded to fluorine but differing in the number of fluorines or in structural arrangement. The ratio of fluorine to total carbon was only slightly lower than the values for the control and vacuum-exposed samples. This result indicates that the ion-texturing process produces a surface only slightly different from the untextured samples.

SUMMARY

An eight-centimeter diameter, electron-bombardment, argon-ion source was used to sputter etch nine biomedical polymers. The materials included silicone rubber (Silastic), 32% carbon-impregnated polyolefin, polyoxymethylene (Delrin), polytetrafluoroethylene (Teflon), ultrahigh molecular weight (UHMW) polyethylene, UHMW polyethylene with carbon fibers (10%), bioelectric polyurethane, segmented polyurethane (Biomer), and crosslinked polyurethane (Tecoflex). Scanning electron microphotographs indicate that the carbon-impregnated polyolefin, bioelectric polyurethane, segmented polyurethane, and cross-linked polyurethane develop a worm-like surface structure as a result of ion sputtering. Polyoxymethylene and polytetrafluoroethylene develop a needle-or cone-like structure. Silicone rubber, UHMW poly-

ethylene, and UHMW polyethylene with carbon fibers did not develop a pronounced surface roughness after ion sputter etching.

The results of tensile tests of microtensile specimens of each polymer indicated a percent reduction in ultimate tensile strength resulting from ion-texturing ranging from 1% for segmented polyurethane to 19% polyoxymethylene. Because of the large range of variation of some of the results, it can be concluded that the reduction of tensile strength after ion-texturing is not a significant change. The general shape of the stress-strain curves for both untextured and ion-textured samples of all the polymers was the same. The two exceptions were polytetrafluoroethylene and polyoxymethylene. Ion-textured polytetrafluoroethylene samples showed a slight change in the stress-strain curves that was similar to the effect of slightly elevating the sample temperature. Ion-textured polyoxymethylene samples did not have a forced low elastic modulus deformation portion which was characteristic of the untextured samples.

ESCA data revealed only minor differences between the untextured control samples and vacuum-exposed samples of each polymer. Therefore, any changes in the near-surface chemical composition after ion-texturing can be attributed to the texturing phenomenon.

All ion-textured samples except 32% carbon-impregnated polyolefin and polytetrafluoroethylene showed detectable amounts of argon on the surface. Silicon was found on all samples before ion-texturing and all samples except polyethylene with 10% carbon fibers and 32% carbon-impregnated polyolefin after ion-texturing.

Among the hydrocarbons UHMW polyethylene became oxidized after ion-sputtering (The oxygen concentration increased and an oxidized carbon peak arose.) UHMW polyethylene with 10% carbon fibers shows an increase in the oxygen content at the expense of the silicon but there is no oxidized carbon peak. The 32% carbon-impregnated polyolefin sample showed an increase in the carbon content relative to the oxygen.

The near-surface chemical composition of the polyurethanes was not drastically changed by the ion beam. Each of the polyurethanes may have been reduced (decrease in oxygen content) by ion bombardment.

Polyoxymethylene showed the most dramatic chemical composition change after ion-texturing. The oxygen content relative to the carbon went from 0.75 for the untextured sample to 0.16 for the ion-textured sample. Polytetrafluoroethylene showed a small increase in the hydrocarbon component after ion-texturing.

In general the ion sputtering effects on surface morphology are more pronounced than the effects on surface chemistry.

ACKNOWLEDGEMENT

I would like to acknowledge the valuable assistance of Dr. Leroy Scharpen, Project Manager, and Patricia Zajicek, Chemist, of Surface Science Laboratories, Inc. of Palo Alto, California; and Dr. David Dwight, Associate Professor, and Betty Beck, graduate student, of Virginia Polytechnic Institute and State University in Blacksburg, Virginia, for their analyses and interpretation of ESCA results. I am also grateful for the assistance of Dr. George Picha, Dr. Donald Gibbons, and Ray Taylor in setting up the tensile testing equipment at Case Western Reserve University.

REFERENCES

1. Szycher, M.; et. al.: Development and Testing of Flocking Materials. NIH-NOL-HV-3-2915-4, National Institute of Health, 1977.
2. Ducheyne, P.; et al.: Influence of a Functional Dynamic Loading on Bone Ingrowth into Surface Pores of Orthopedic Implants. J. Biomed. Mater. Res., vol. 11, no. 6, Nov. 1977, pp. 811-838.
3. Spector, M.; Kreuter, A.; and Sauer, B. W.: Scanning Electron Microscopy of the Healing Response to Porous Orthopedic and Dental Implants. Scanning Electron Microscopy, 1976, II. O. Johari and R. P. Becker, eds., Vol. II, Pt. V, IIT Research Institute, 1976, pp. 299-306.
4. Nose, Y.; et al.: Development and Evaluation of Cardiac Prostheses. NIH-NOL-HV-4-2960-2, National Institute of Health, 1976.
5. Banks, B. A.; et al.: Potential Biomedical Applications of Ion Beam Technology. NASA TM X-73512, 1976.
6. Weigand, A. J.; and Banks, B. A.: Ion-Beam-Sputter Modification of the Surface Morphology of Biomedical Implants. J. Vac. Sci. Technol., vol. 14, no. 1, Jan.-Feb. 1977, pp. 326-331.
7. Weigand, A. J.: Mechanical Properties on Ion Beam Textured Surgical Implant Alloys. J. Vac. Sci. Technol., vol. 15, no. 2, Mar.-Apr. 1978, pp. 718-724.

8. Weigand, A. J.: The Use of an Ion-Beam Source to Alter the Surface Morphology of Biomedical Implant Materials. NASA TM X-78851, 1978.
9. Hudson, W. R.: Nonpropulsive Application of Ion Beams. AIAA paper 76-1015, Nov. 1976.
10. Matlaga, B. F.; YASENCHAK, L. P.; and Salthouse, T. N.: Tissue Response to Implanted Polymers: The Significance of Sample Shape. *J. Biomed. Mat. Res.*, vol. 10, no. 3, May 1976, pp. 391-397.
11. Yasuda, H.; Yamanashi, B. S.; and Devito, D. P.: The Rate of Adhesion of Melanoma Cells onto Nonionic Polymer Surfaces. *J. Biomed. Mat. Res.*, vol. 12, no. 5, Sep. 1978, pp. 701-706.
12. Kaufman, H. R.; and Robinson, R. S.: Industrial Ion Source Technology. (Colorado State Univer.; NASA Grant NSG-3086). NASA CR-159534, 1978.
13. Kerslake, W. R.; and Banks, B. A.: Evolution of the 1-mlb Mercury Ion Thruster Subsystem. NASA TM X-73733, 1978.
14. Dwight, D. W.: Monthly Report for NASA Grant NSG-3204, Virginia Polytechnic Inst. and State Univer., March 1979.
15. ESCA Analytical Service Report. Rep. 22-878, Surface Science Laboratories, 1978.
16. Mechanical Properties of Polymers, Encyclopedia Reprints. Norbert M. Bikales, ed., Wiley-Interscience, 1971, p. 18.
17. Fluoropolymers. Leo A. Wall, ed., Wiley-Interscience, 1972, pp. 526-530.

TABLE I. - SAMPLE MATERIAL THICKNESS AND ION CURRENT DENSITY IMPINGING ON EACH POLYMER

[Argon ion beam energy, 500 eV; target distance from ion source, 20 cm; ion-texturing duration, 1 hr.]

Material	Ion-beam current density, mA/cm ²	Average sample thickness, mm
Bioelectric polyurethane	0.10	0.66
Segmented polyurethane	.19	.51
Polyoxymethylene	.08	.81
Ultra high molecular weight (UHMW) polyethylene	.19	3.18
UHMW polyethylene with 10% carbon fibers	.19	3.18
32% Carbon-impregnated polyolefin	.10	1.12
Cross-linked polyurethane	.10	.76
Polytetrafluoroethylene	.19	.25

TABLE II. - TENSILE TEST RESULTS OF UNTEXTURED AND ION-TEXTURED POLYMERS

Material	Sample surface condition**	Number of samples	Average tensile strength at failure		Percent range of variation $(\max - \min) \times 100$ avg	Percent loss of tensile strength between untextured and ion-textured samples	Crosshead speed	
			N/M ² x 10 ⁻⁷	psi			mm/min	(in./min)
Bioelectric polyurethane	U	4*	2.22	3220	26	3.0	125	5
	T	5	2.15	3120	12			
Segmented polyurethane (Biomer)	U	5	4.07	5910	7	1.3	500	20
	T	2*	4.01	5830	2			
Polyoxymethylene (Delrin)	U	4*	6.34	9200	6	19.4	5	0.2
	T	5	5.01	7420	15			
32% Carbon-impregnated polyolefin	U	4*	1.61	2340	4	13.3	125	5
	T	4*	1.39	2020	20			
Butadiene rubber (elastomeric)	U	5	0.76	1100	28	9.6	500	20
	T	5	0.68	990	19			
Cross-linked polyurethane (Tecoflex)	U	3*	2.67	3880	10	15	500	20
	T	3*	2.26	3290	50			
Polytetrafluoroethylene (Teflon)	U	5	3.18	4680	11	18	50	2
	T	5	2.64	3830	34			

*Not equal to 5 because sample(s) slipped out of grip prior to failure.

**U = Untextured; T = Ion-textured.

TABLE III. - SURFACE ELEMENTAL COMPOSITION EXPRESSED AS ATOM PERCENT FOR THE DETECTED ELEMENTS

Samples	Elements													
	C	O	N	Si	Na	Mg	Fe	Zn	Sn	Ca	Ir	P	S	Cl
Bioelectric polyurethane:														
Control	74	20	1.4	4.7	-----	-----	-----	-----	-----	-----	-----	-----	-----	-----
Vacuum	72	20	.9	6.3	-----	-----	-----	-----	-----	-----	0.6	-----	-----	-----
Ion-textured	79	15	.5	4.2	-----	-----	-----	-----	-----	-----	<.1	0.4	-----	0.4
Segmented polyurethane:														
Control	72	19	2.1	5.5	-----	0.2	-----	-----	-----	-----	-----	.5	.5	0.2
Vacuum	71	20	2.9	4.7	0.04(?)	.2	-----	-----	-----	-----	-----	.3	.6	-----
Ion-textured	85	11	1.8	1.2	.15	<.03	-----	-----	-----	-----	-----	.09	-----	.4
Polyoxymethylene:														
Control	57	37	1.5	3.2	-----	-----	-----	0.3	-----	-----	-----	.2	.3	-----
Vacuum	57	43	1.1	1.1	-----	-----	-----	-----	-----	-----	-----	.03	-----	-----
Ion-textured	85	14	1.2	1.2	-----	-----	-----	.5	-----	-----	-----	-----	-----	.1
Polyethylene:														
Control	81	12	.2	5.4	.7	0.7	-----	-----	-----	-----	-----	.7	-----	-----
Vacuum	88	8.2	---	3.1	---	.3	-----	-----	-----	-----	-----	.5	-----	-----
Ion-textured	73	17	.7	5.5	.1	1.5	-----	1.0	-----	-----	-----	.6	.3	.2
Polyethylene with 10% carbon fibers:														
Control	87	7.6	.4	3.7	-----	.4	-----	-----	-----	-----	-----	.3	.2	-----
Vacuum	83	9.2	.7	5.1	-----	1.2	-----	-----	-----	-----	-----	.3	.3	-----
Ion-textured	86	12	.4	.5	-----	.8	-----	-----	-----	-----	-----	.1	.2	-----
32% Carbon impregnated polyolefin:														
Control	85	8.2	.4	4.5	-----	-----	.2	-----	-----	-----	-----	1.6	.8	.2
Vacuum	83	8.2	.7	3.6	-----	-----	.4	-----	-----	-----	-----	3.1	.6	.07
Ion-textured	95	2.8	---	---	---	---	.4	-----	-----	-----	-----	.1	1.3	-----
Silicone rubber:														
Control	50	23	---	---	---	---	---	---	---	---	---	---	---	---
Vacuum	48	24	---	28	---	---	---	---	---	---	---	---	---	---
Ion-textured	51	25	---	23	---	---	---	---	---	---	---	---	---	---
Cross-linked polyurethane:														
Control	75	19	1.5	3.8	-----	-----	0.04	-----	-----	1.0	-----	-----	-----	-----
Vacuum	66	18	1.9	3.4	-----	-----	-----	.68	-----	-----	11.1	-----	-----	-----
Ion-textured	84	13	.7	2.0	-----	-----	-----	.06	-----	-----	<.06	-----	-----	.3
Polytetrafluoroethylene:														
Control	34	7	---	5	---	---	---	---	---	---	65	-----	-----	-----
Vacuum	35	1.2	---	2	---	---	---	---	---	---	64	-----	-----	-----
Ion-textured	39	1.0	---	.2	---	---	---	---	---	---	60	-----	-----	-----

Note: Values followed by ? indicate a weak signal from the element was possibly present but it was close to the detection limits; < indicates no signal was observed but an upper limit was calculated from the data; --- indicates no observation of a signal.

ORIGINAL PAGE
OF POOR QUALITY

TABLE IV. - SURFACE ELEMENTAL COMPOSITION EXPRESSED AS NUMBER OF ATOMS RELATIVE TO TOTAL CARBON DEFINED AS 1.00

[C_a binding energy < C_b binding energy < C_c binding energy < Cd binding energy.]

Samples	Elements							
	C-H or C _a	C-C C _b	C=O C _c	C-F C _d	O	N	Si	P
Bioelectric polyurethane:								
Control	0.54	0.43	0.03	-----	0.27	0.018	0.064	-----
Vacuum	.60	.37	.03	0.006	.27	.013	.087	0.009
Ion-textured	.71	.25	.04	-----	.19	.0069	.054	<.001
Segmented polyurethane:								
Control	.74	.19	.07	-----	.26	.028	.077	.007
Vacuum	.72	.19	.09	-----	.29	.041	.067	-----
Ion-textured	.72	.23	.05	-----	.12	.021	.014	-----
Polyoxymethylene:								
Control	.38	.62	-----	-----	.64	-----	.05	-----
Vacuum	.23	.77	-----	-----	.75	-----	.042	-----
Ion-textured	.86	.06	.08	-----	.16	-----	.002	-----
Polyethylene:								
Control	.97	.03	-----	-----	.14	-----	.066	-----
Vacuum	.98	.02	-----	-----	.09	-----	.035	-----
Ion-textured	.90	.10	-----	-----	.23	-----	.075	-----
Polyethylene with 10 ⁸ carbon fibers:								
Control	1.00	-----	-----	-----	.09	-----	.042	-----
Vacuum	1.00	-----	-----	-----	.11	-----	.060	-----
Ion-textured	1.00	-----	-----	-----	.14	-----	.006	-----
3.2% Carbon impregnated polyolefin:								
Control	1.00	-----	-----	-----	.097	-----	.53	-----
Vacuum	1.00	-----	-----	-----	.062	-----	-----	-----
Ion-textured	1.00	-----	-----	-----	.028	-----	-----	-----
Silicone rubber:								
Control	1.00	-----	-----	-----	.47	-----	.53	-----
Vacuum	1.00	-----	-----	-----	.49	-----	.58	-----
Ion-textured	1.00	-----	-----	-----	.50	-----	.45	-----
Cross-linked polyurethane:								
Control	.59	.39	.02	-----	.26	.020	.052	.01
Vacuum	.62	.35	.04	-----	.27	.029	.051	.17
Ion-textured	.72	.26	.03	-----	.16	.009	.024	-----
Polytetrafluoroethylene:								
Control	.06	.94	-----	-----	.02	-----	.014	1.95
Vacuum	.12	.88	-----	-----	.04	-----	.005	1.84
Ion-textured	.08	.88	.08	.76	.03	-----	.005	1.52

TABLE V. - BINDING ENERGIES OF PHOTOELECTRON PEAKS FROM HIGH-RESOLUTION SPECTRA
NORMALIZED TO PUT C_a(1s) at 284.0 eV

Samples	Elements								
	C _a	C _b	C(1s)	C _c	C _d	O(1s)	N(1s)	Si(2p)	F(1s)
Bioelectric polyurethane:	284.0	285.4	287.6	291.4	531.7	398.9	101.1	688.1	688.1
Control	285.4	286.8	291.4	531.6	398.6	101.1	688.1	688.1	688.1
Vacuum	285.6	287.6	291.8	531.8	399.4	101.8	688.1	688.1	688.1
Segmented polyurethane:	285.5	287.7	291.7	531.5	398.6	101.5	688.1	688.1	688.1
Control	285.6	287.7	291.8	531.6	398.9	102.1	688.1	688.1	688.1
Vacuum	285.4	287.8	291.5	531.5	398.3	101.2	688.1	688.1	688.1
Ion-textured polyoxymethylene:	287.0	287.0	287.1	532.1	398.1	101.1	688.1	688.1	688.1
Control	286.9	288.1	288.0	532.0	398.0	101.1	688.1	688.1	688.1
Vacuum	286.1	288.1	288.1	531.8	398.0	101.1	688.1	688.1	688.1
Polyethylene:	288.0	288.0	288.0	531.3	398.3	101.3	688.1	688.1	688.1
Control	288.3	287.5	287.5	531.6	398.6	101.3	688.1	688.1	688.1
Vacuum	287.5	287.5	287.5	531.3	398.0	101.0	688.1	688.1	688.1
Polyethylene with 10% carbon fibers:	287.5	287.5	287.5	531.5	398.5	101.4	688.1	688.1	688.1
Control	287.5	287.5	287.5	531.4	398.4	101.1	688.1	688.1	688.1
Vacuum	287.5	287.5	287.5	531.7	398.7	101.2	688.1	688.1	688.1
32% Carbon impregnated polyolefin	287.5	287.5	287.5	531.6	398.6	101.6	688.1	688.1	688.1
Control	287.5	287.5	287.5	531.4	398.4	101.4	688.1	688.1	688.1
Vacuum	287.5	287.5	287.5	531.4	398.7	101.5	688.1	688.1	688.1
Silicone rubber:	287.5	287.5	287.5	531.6	398.6	101.6	688.1	688.1	688.1
Control	287.5	287.5	287.5	531.5	398.5	101.4	688.1	688.1	688.1
Vacuum	287.5	287.5	287.5	531.6	398.8	101.5	688.1	688.1	688.1
Cross-linked polyurethane:	285.4	288.1	287.7	531.7	399.0	101.2	688.6	688.6	688.6
Control	285.3	287.8	287.4	531.7	399.1	101.4	688.6	688.6	688.6
Vacuum	285.6	288.2	287.8	531.8	398.9	101.3	688.6	688.6	688.6
Polytetrafluoroethylene:	291.4	291.5	291.4	531.4	398.4	101.4	688.9	688.9	688.9
Control	291.5	288.4	290.8	531.6	398.6	101.6	689.0	689.0	689.0
Vacuum	286.1	288.4	290.8	531.4	398.4	101.4	688.4	688.4	688.4
Ion-textured									

*Note = Si(2s) binding energy for samples 6a and 6b.

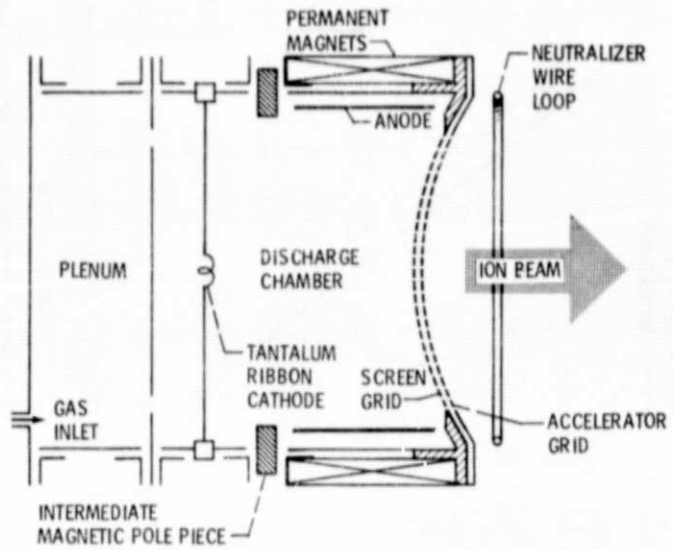


Figure 1. - Cross section of ion-beam source.

E-152

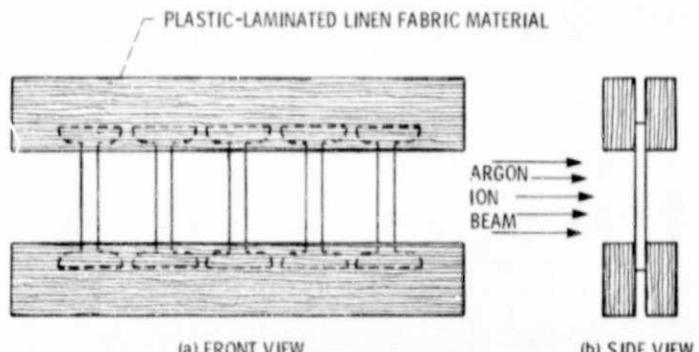


Figure 2. - Ion-sputtering of microtensile specimens.

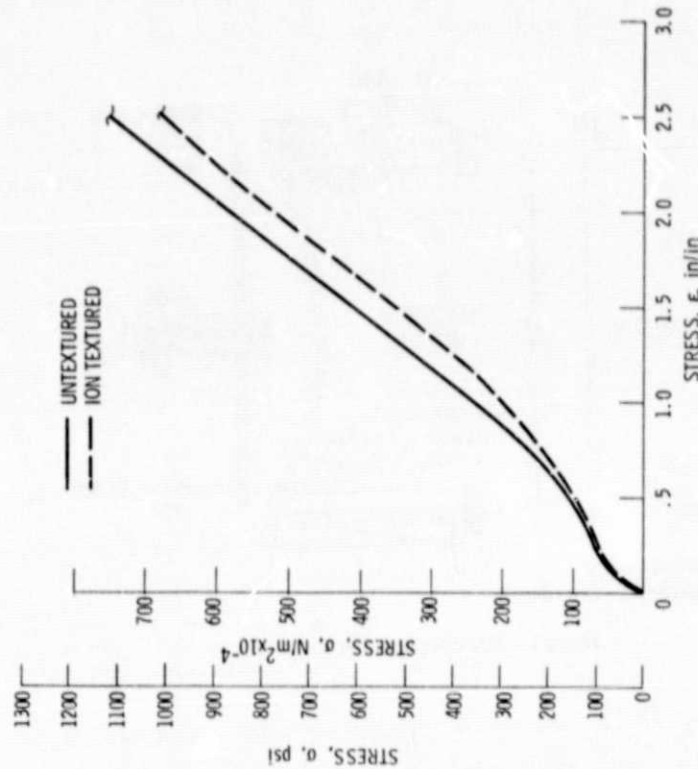


Figure 4. - Stress-strain diagram for untextured and ion-textured silicone rubber.

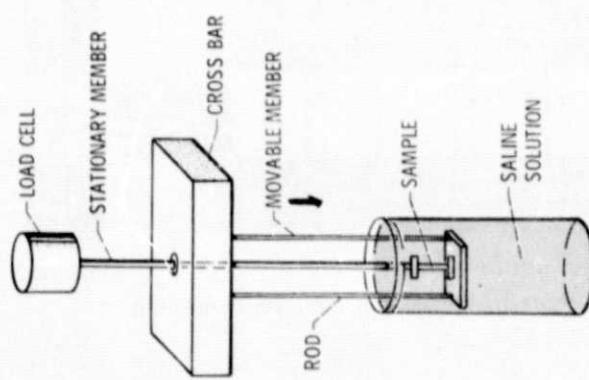


Figure 3. - Tensile test apparatus.

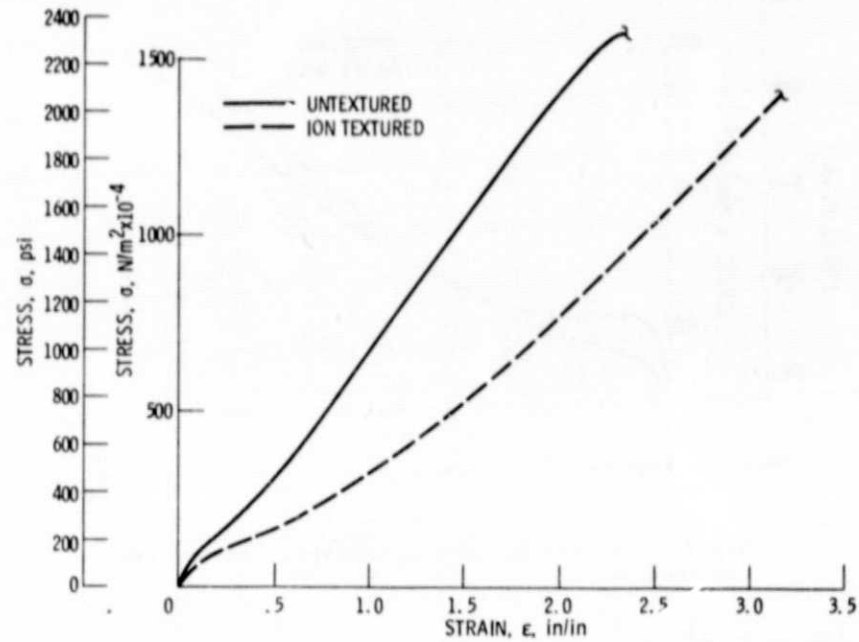


Figure 5. - Stress-strain diagram for untextured and ion-textured 32 percent carbon-impregnated polyolefin.

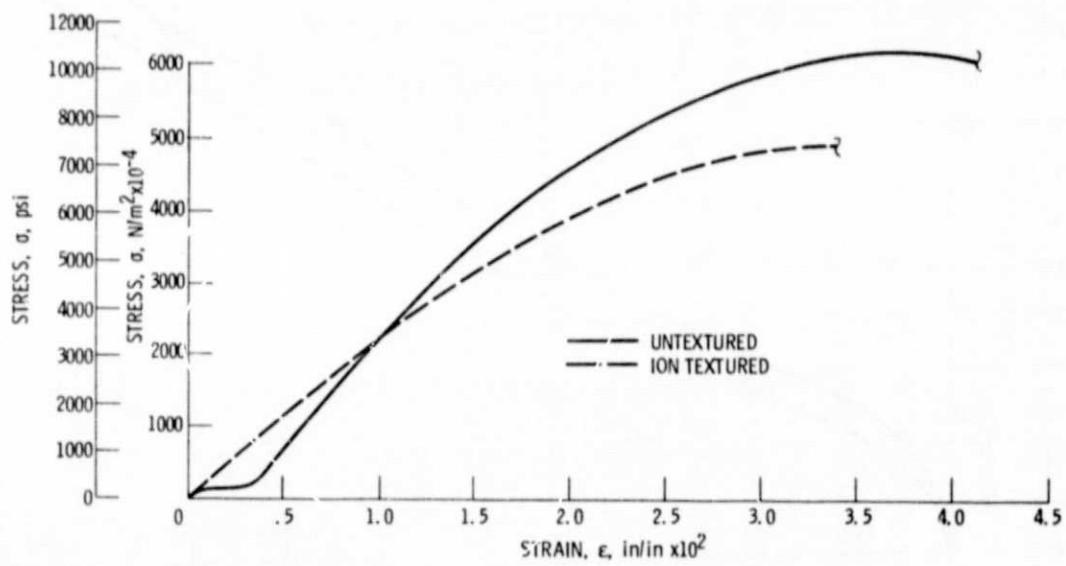


Figure 6. - Stress-strain diagram for untextured and ion-textured polyoxymethylene.

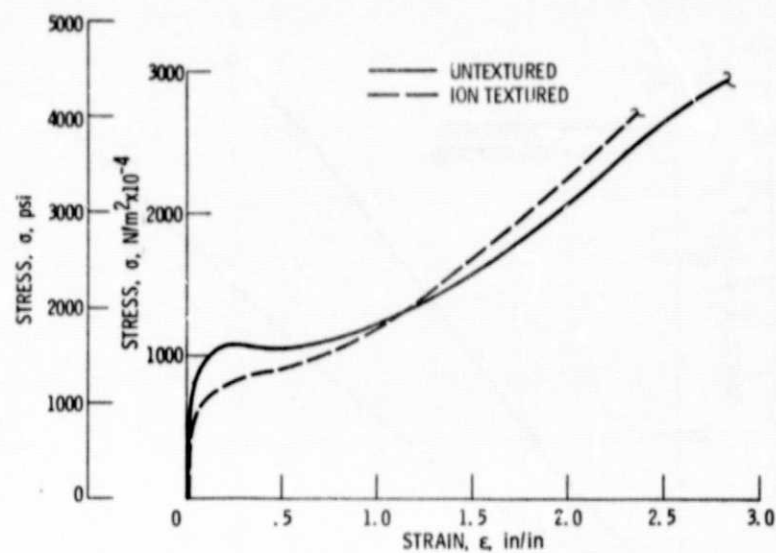


Figure 7. - Stress-strain diagram of untextured and ion-textured polytetrafluoroethylene.

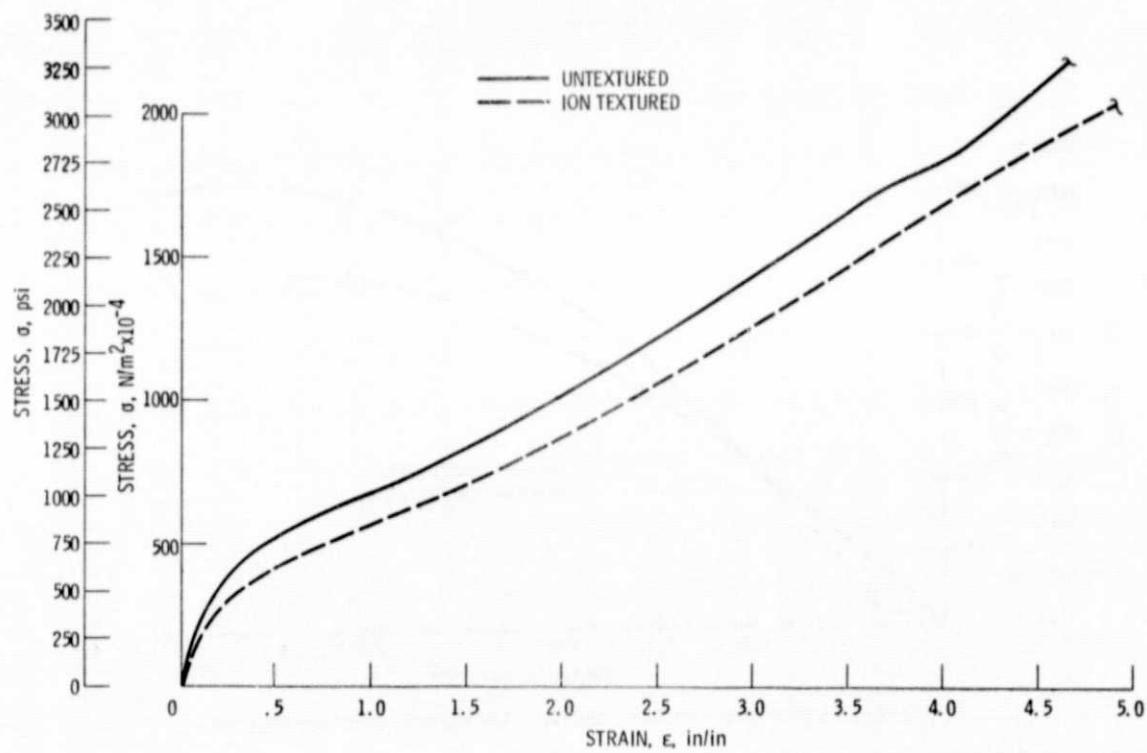


Figure 8. - Stress-strain diagram of untextured and ion-textured bioelectric polyurethane.

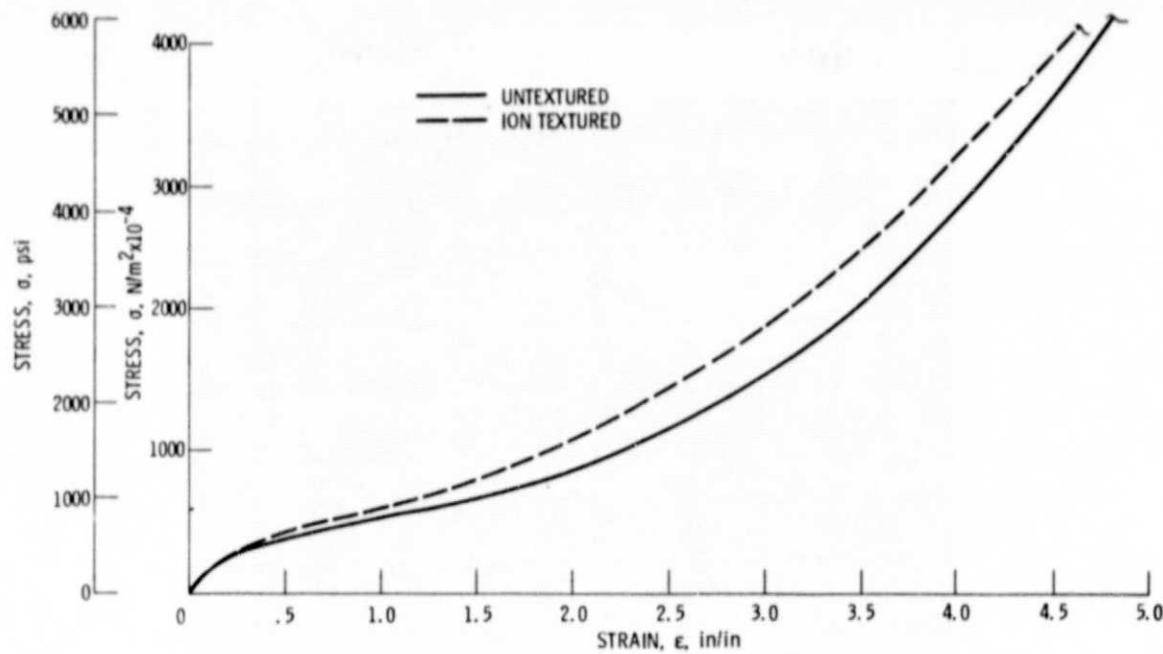


Figure 9. - Stress-strain diagram of untextured and ion-textured segmented polyurethane.

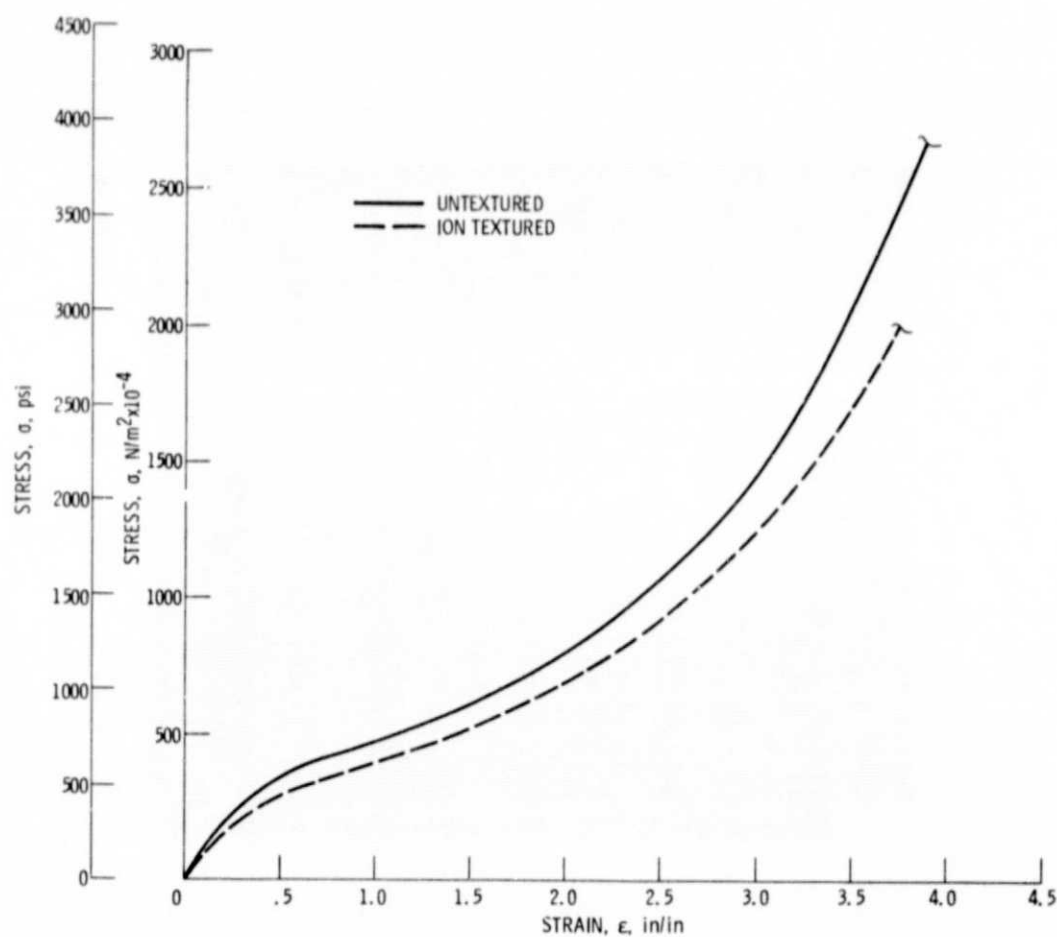


Figure 10. - Stress-strain diagram of untextured and ion-textured cross-linked polyurethane.

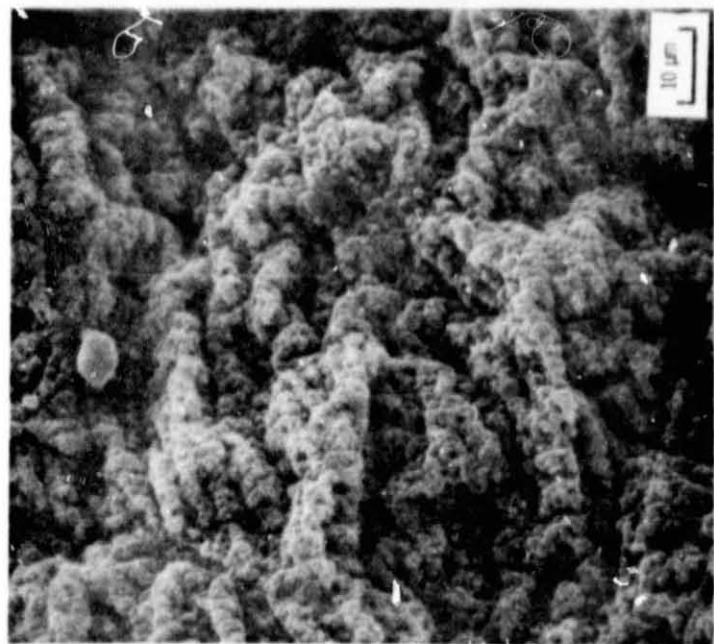


Figure 12. - Argon-ion textured 32% carbon-impregnated polyolefin. 1000X.

CS-78-1362

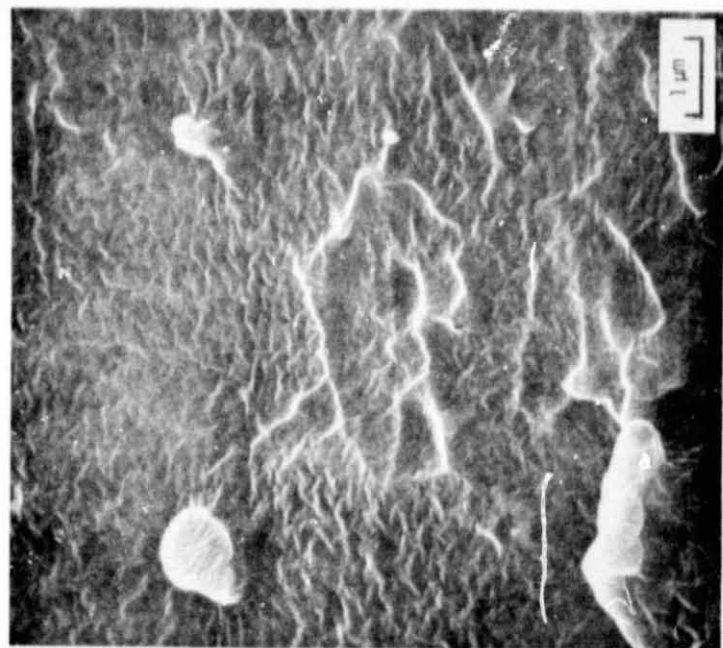


Figure 11. - Argon-ion textured silicone rubber. 3000X.

CS-78-1370

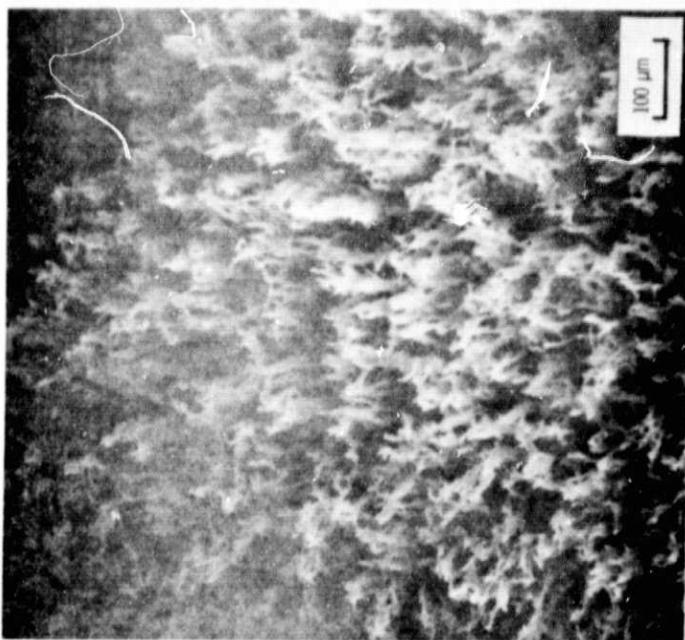


Figure 13. - Argon-ion textured poly(1,1,2,2-tetrafluoroethylene), 100X.

CS-78-1365

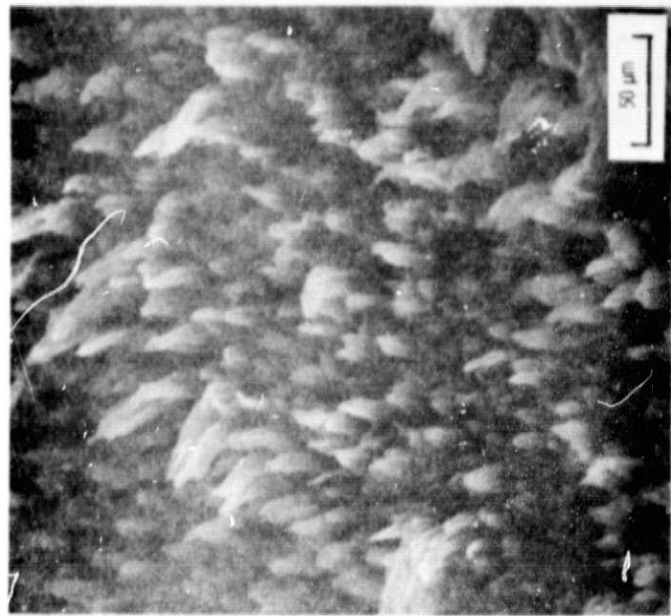


Figure 14. - Argon-ion textured polytetrafluoroethylene, 3000X.

CS-78-1364

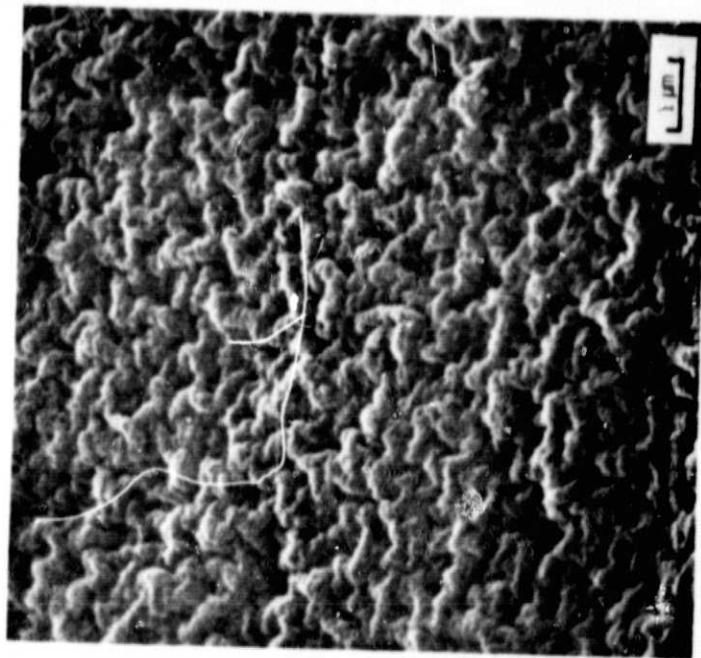


Figure 16. - Argon-ion textured segmented polyurethane, 10,000X.

C5-78-1369

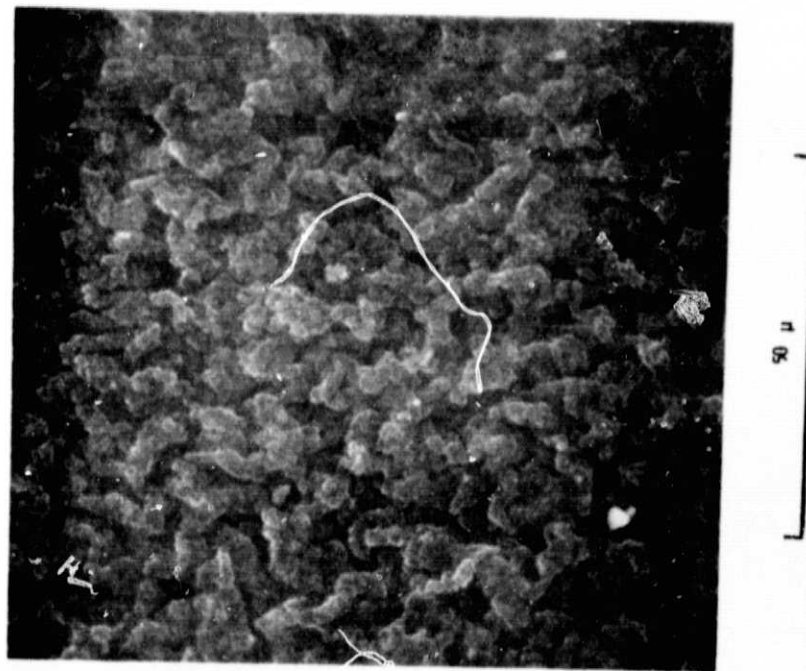


Figure 15. - Argon-ion textured bioelectric polyurethane, 1000X.

E-152

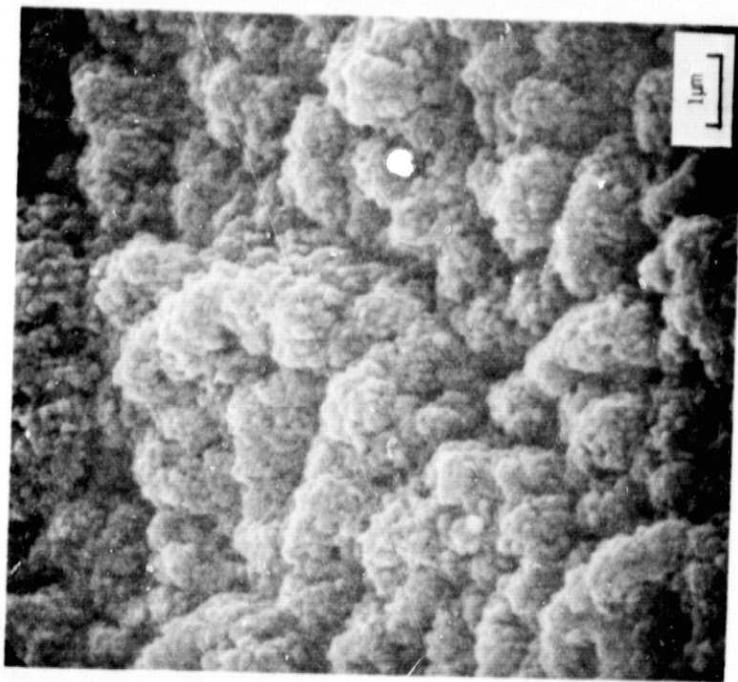


Figure 17. - Argon-ion textured cross-linked polyurethane, 10,000X.

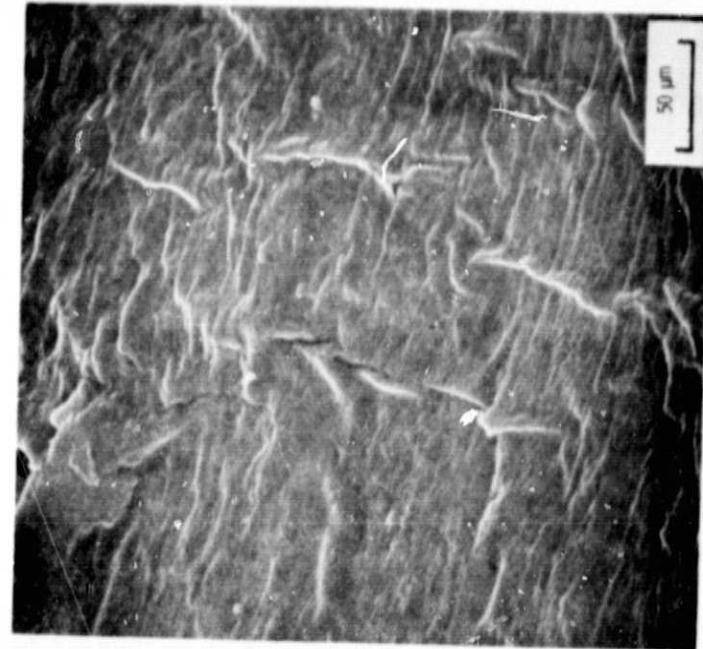


Figure 18. - Argon-ion textured high molecular weight polyethylene, 3000X.

CS-78-1363



Figure 19. - Argon-ion textured high-molecular weight polyethylene with 10% carbon fibers, 300X.

ORIGINAL PAGE IS
OF POOR QUALITY